

On the Performance of RIS-assisted Networks with HQAM

Thrassos K. Oikonomou*, Dimitrios Tyrovolas*, Sotiris A. Tegos*[†],

Panagiotis D. Diamantoulakis*, Panagiotis Sarigiannidis[†], Christos Liaskos[‡], George K. Karagiannidis*[§]

*Department of Electrical and Computer Engineering, Aristotle University of Thessaloniki, 54124 Thessaloniki, Greece

e-mail: {toikonom, tyrovolas, tegosoti, padiaman, geokarag}@auth.gr

[†]Department of Electrical and Computer Engineering, University of Western Macedonia, 50100, Kozani, Greece

e-mail: psarigiannidis@uowm.gr

[‡]Computer Science Engineering Department, University of Ioannina, Ioannina, Greece. e-mail: cliaskos@ics.forth.gr

[§]Artificial Intelligence & Cyber Systems Research Center, Lebanese American University (LAU), Lebanon

Abstract—In this paper, we investigate the application of hexagonal quadrature amplitude modulation (HQAM) in reconfigurable intelligent surface (RIS)-assisted networks, specifically focusing on its efficiency in reducing the number of required reflecting elements. Specifically, we present analytical expressions for the average symbol error probability (ASEP) and propose a new metric for conditioned energy efficiency, which assesses the network's energy consumption while ensuring the ASEP remains below a certain threshold. Additionally, we introduce an innovative detection algorithm for HQAM constellations that implements sphere decoding in $\mathcal{O}(1)$ complexity. Finally, our study reveals that HQAM significantly enhances both the ASEP and energy efficiency compared to traditional quadrature amplitude modulation (QAM) schemes.

Index Terms—HQAM, Reconfigurable Intelligent Surfaces (RISs), Energy Efficiency, Average Symbol Error Probability, Detection Algorithm

I. INTRODUCTION

Motivated by the rise of innovative applications such as extended reality, smart industries, and autonomous vehicles, there is a growing demand to enhance the capabilities of wireless networks [1]. In this direction, a new wireless communication paradigm has emerged, named programmable wireless environment (PWE), aiming to transform the wireless propagation phenomenon into a software-defined process [2]. This transformation necessitates coating propagation environments with reconfigurable intelligent surfaces (RISs), which are planar structures capable of modifying the characteristics of the waves impinging upon them, including their direction and polarization [3]. In more detail, RISs can be appropriately configured to improve the quality of the wireless channels, as well as direct intelligently signal propagation to reduce power losses which is crucial for the sustainability of future 6G networks [4]. Thus, RISs can ensure seamless connectivity for demanding futuristic applications but also enhance the network's energy efficiency, paving the way for ubiquitous ultra-reliable green communications.

To reliably perform various RIS functionalities, it is recognized that a significant number of reflecting elements is essential. However, considering that each element contributes to the network's power consumption through the tuning mechanism of their impedance, it becomes imperative to expand the capabilities of digital communication systems to ensure reliable performance with as few reflecting elements as pos-

sible. Within this context, hexagonal quadrature amplitude modulation (HQAM) stands out as a novel modulation scheme, due to its efficient and compact allocation of symbols on the 2D plane [5], [6]. Specifically, HQAM represents an appropriate modulation scheme for applications that prioritize energy savings, owing to its hexagonal lattice's ability to maximize the use of available space, thereby leading to a reduction in energy consumption. In this direction, by taking into account the advantages of HQAM, the authors of [5] provided a comprehensive comparison of HQAM over existing QAM constellations and justify its supremacy in terms of symbol error rate and energy efficiency. Furthermore, the authors of [6] provided a tight closed-form approximation for the symbol error probability of HQAM, as well as a detection algorithm for HQAM constellations of $\mathcal{O}(\log\sqrt{M})$ complexity. Finally, [7] investigated the effects of outdated channel state information, pointing errors, and atmospheric turbulence on the average symbol error probability (ASEP) for a mixed FSO/RF system that utilizes HQAM. However, to the best of the authors' knowledge, there exists no work that quantifies the effect of HQAM in an RIS-assisted network, particularly in terms of reducing the number of reflecting elements.

In this work, we analyze the performance of an RIS-assisted network that utilizes HQAM scheme, focusing on its potential to reduce the number of reflecting elements required for maintaining high-quality communication. Specifically, we derive analytical expressions for the ASEP and introduce a novel metric named conditioned energy efficiency, which evaluates the network energy efficiency while keeping the ASEP below a predefined threshold. Furthermore, we propose a novel detection algorithm for HQAM that implements sphere decoding in $\mathcal{O}(1)$ complexity, thereby enhancing the practical applicability of HQAM in future wireless communication systems. Finally, our simulation results reveal that HQAM offers significant improvements in the ASEP and the energy efficiency of RIS-assisted networks over traditional QAM schemes.

II. SYSTEM MODEL

We consider an uplink communication network that consists of a single-antenna base station (BS) and a single antenna

communication node (CN). Due to the harsh wireless propagation environment, it is assumed that there is no direct communication link available to facilitate the connection between the CN and BS. To enhance the received power at the BS, we employ a RIS with N reflecting elements which assists the CN-BS communication by steering the CN transmissions towards the BS. Therefore, considering the RIS reflection path, the baseband equivalent of the received symbol at the BS can be expressed as

$$y = \sqrt{P_t G l_p} \sum_{i=1}^N |h_{i1}| |h_{i2}| e^{(\omega_i + \arg\{h_{i1}\} + \arg\{h_{i2}\})} s + w, \quad (1)$$

where s is the transmitted symbol from a constellation \mathcal{C} with unitary average energy, i.e., $\mathbb{E}[|E_s|] = \mathbb{E}[|s|^2] = 1$ where $\mathbb{E}[\cdot]$ denotes the expectation of a random variable (RV), while $|\cdot|$ and $\arg\{\cdot\}$ denote the magnitude and the argument of a complex number, respectively. Also, P_t is the transmit power, $G = G_t G_r$ denotes the product of the CN and AP antenna gains, and h_{1i} and h_{2i} are the complex channel coefficients that correspond to the links between the CN and the i -th reflecting element and between the i -th reflecting element and the BS, respectively. More precisely, the RVs $|h_{1i}|$ and $|h_{2i}|$ are assumed to follow Nakagami- m distribution with shape parameter m and spread parameter Ω , which can describe accurately realistic communication scenarios characterized by severe or light fading. Moreover, w is the complex additive white Gaussian noise (AWGN) with zero mean and standard deviation $\sigma_n^2 = N_0$, ω_i is the phase correction term induced by the i -th element, and l_p is the path loss corresponding to the CN-RIS-BS link. Specifically, l_p can be modeled as $l_p = C_0^2 \left(\frac{d_0}{d_1 d_2}\right)^n$, where n expresses the path loss exponent, C_0 denotes the path loss of CN-RIS and RIS-BS links at the reference distance d_0 , while d_1 and d_2 denote the distances of the CN-RIS and RIS-BS links, respectively.

To maximize the signal-to-noise ratio (SNR) at the receiver, the phase shift of the i -th reflecting element ω_i is ideally chosen to nullify the combined phase shift $\arg\{h_{i1}\} + \arg\{h_{i2}\}$ [3]. However, considering the reflecting elements' impedance being controlled by q PIN diodes, there are 2^q distinct patterns of phase shifts for each element. Therefore, the received signal y can be rewritten as

$$y = \sqrt{P_t G l_p} h s + w, \quad (2)$$

where $h = \sum_{i=1}^N |h_{1i}| |h_{2i}| e^{\phi_i}$, and ϕ_i is a uniformly distributed RV over $[-2^{-q}\pi, 2^{-q}\pi]$ [8]. Finally, by assuming perfect channel state information (CSI) knowledge, the received symbol r can be obtained by performing channel inversion.

III. PERFORMANCE ANALYSIS

In this section, we extract analytical expressions for the examined network's ASEP and introduce a new metric named conditioned energy efficiency, which quantifies the ratio of the throughput to the network's energy consumption under the condition that ASEP remains below a predefined threshold.

The Symbol Error Probability (SEP) stands as one of the most crucial metrics for assessing the performance of

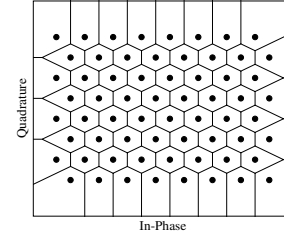


Fig. 1: 64-HQAM constellation

TABLE I: Parameter k_c for M -HQAM.

M	16	64	256	1024
k	0.8711505	0.5222431	0.3936315	0.2982858

a modulation scheme. However, due to HQAM hexagonal lattices as shown in Fig. 1, evaluating the exact SEP is challenging. Therefore, by approximating the area of the regular hexagons with a circle as shown in [6], the SEP can be tightly approximated as

$$P_s(\gamma_r, k_c) \approx \frac{2M-b}{2M} e^{-\gamma_r B} + \frac{b}{M} Q(\sqrt{\gamma_r} A), \quad (3)$$

where $Q(x) = \frac{1}{\sqrt{2\pi}} \int_x^\infty \exp\left(-\frac{u^2}{2}\right) du$ is the Gaussian Q -function, γ_r is the received SNR, $B = \frac{d_{\min}^2 k_c^2}{3E_s} + \frac{d_{\min}^2 k_c(1-k_c)}{\sqrt{3}E_s} + \frac{d_{\min}^2(1-k_c)^2}{4E_s}$ and $A = \sqrt{\frac{2d_{\min}^2 k_c^2}{3E_s}} + \sqrt{\frac{d_{\min}^2(1-k_c)^2}{2E_s}}$, respectively. Moreover, d_{\min} denotes the nearest-neighbour distance and is expressed as

$$d_{\min} = \sqrt{\frac{12E_s}{7M-4}}, \quad (4)$$

and b denotes the number of the constellation's external symbols [6]. Finally, by taking into account the constellation order M , the values of k_c is given in Table I. However, considering the existence of fading channels in the examined scenario, it is imperative to derive the probability density function (PDF) $f_{|h|}(\cdot)$ of $|h|$, to derive the ASEP of the considered RIS-assisted network. To this end, we provide a closed-form expression that tightly approximates the PDF of the considered channel h .

Proposition 1: The PDF of $|h|$ for the considered RIS-assisted network can be tightly approximated as

$$f_{|h|}(x) \approx \frac{2m_t^{m_t}}{\Gamma(m_t)\Omega_t^{m_t}} x^{2m_t-1} e^{-\frac{m_t x^2}{\Omega_t}}, \quad (5)$$

where $\Gamma(\cdot)$ is the gamma function, $m_t = \frac{I_1^2}{I_2 - I_1^2}$, $\Omega_t = I_1^2$ and I_1, I_2 are given by (6) and (7) at the top of the next page, respectively.

Proof: Considering that N is large, by applying the moment-matching technique [9], $|h|^2$ can be approximated as a gamma-distributed RV with scale parameter $k_t = \frac{I_1^2}{I_2 - I_1^2}$ and shape parameter $\theta_t = \frac{I_2 - I_1^2}{I_1^2}$, where I_1 and I_2 are the first and the second moment of $|h|^2$, hence $|h|$ can be approximated as a Nakagami- m RV with shape parameter $m_t = k_t$ and scale parameter $\Omega_t = k_t \theta_t$. Therefore, to tightly approximate

$$I_1 = N \left(\Omega^2 + (N-1) \left(\frac{2^q \Omega \sin(\frac{\pi}{2^q}) \Gamma(m + \frac{1}{2})}{m\pi \Gamma(m)} \right)^2 \right) \quad (6)$$

$$\begin{aligned} I_2 = & N(N-1)(N-2)(N-3) \left(\frac{\Gamma(m + \frac{1}{2})}{\Gamma(m)} \right)^8 \frac{\Omega^4}{m^4} \frac{2^{4q}}{\pi^4} \sin^4\left(\frac{\pi}{2^q}\right) + 4N(N-1) \left(\frac{\Gamma(m + \frac{3}{2})}{\Gamma(m)} \right)^2 \frac{\Omega^3}{m^3} \frac{4^q}{\pi^2} \sin^2\left(\frac{\pi}{2^q}\right) \\ & + N(N-1)(N-2)\Omega^2 \left(\frac{\Gamma(m + \frac{1}{2})}{\Gamma(m)} \right)^4 \frac{\Omega^2}{m^2} \left(\frac{2^{2q+1}}{\pi^2} \sin^2\left(\frac{\pi}{2^q}\right) + 4 \left(\frac{1}{2} + \frac{2^{q-2}}{\pi} \sin\left(\frac{\pi}{2^{q-1}}\right) \right) \frac{4^q}{\pi^2} \sin^2\left(\frac{\pi}{2^q}\right) \right) \\ & + N \left(\frac{\Gamma(m+2)}{\Gamma(m)} \right)^2 \frac{\Omega^4}{m^4} + N(N-1) \left(\Omega^4 + \Omega^4 \left(1 + \frac{2^{2q-2}}{\pi^2} \sin^2\left(\frac{\pi}{2^{q-1}}\right) \right) \right) \end{aligned} \quad (7)$$

$f_{|h|}(x)$, we need to calculate I_1 and I_2 , which are equal to $\mathbb{E}[|h|^2]$, and $\mathbb{E}[|h|^4]$, respectively. Initially, after some algebraic manipulations, $|h|^2$ and $|h|^4$ can be expressed respectively as

$$|h|^2 = \sum_{i=1}^N \sum_{j=1}^N |h_{1i}| |h_{2i}| |h_{1j}| |h_{2j}| \cos(\phi_i - \phi_j), \quad (8)$$

and

$$\begin{aligned} |h|^4 = & \sum_{i=1}^N \sum_{j=1}^N \sum_{k=1}^N \sum_{l=1}^N |h_{1i}| |h_{2i}| |h_{1j}| |h_{2j}| |h_{1k}| |h_{2k}| \\ & \times |h_{1l}| |h_{2l}| \cos(\phi_i - \phi_j) \cos(\phi_k - \phi_l). \end{aligned} \quad (9)$$

By observing (8) and (9), it becomes evident that I_1 and I_2 will consist of N^2 and N^4 terms, respectively. In more detail, considering that $\mathbb{E}[\cdot]$ is a linear operator, $\mathbb{E}[|h|^2]$ and $\mathbb{E}[|h|^4]$ are equal to the sum of the mean values of each term of the summation. To this end, by identifying the expression of each term and calculating its mean value, we can obtain I_1 and I_2 . In this direction, for the case of I_1 , the summation terms are the following:

- $N^2 - N$ terms: $|h_{1i}| |h_{2i}| |h_{1j}| |h_{2j}| \cos(\phi_i - \phi_j)$, if $i \neq j$,
- N terms: $|h_{1i}|^2 |h_{2i}|^2$, if $i = j$.

Therefore, I_1 can be expressed as

$$\begin{aligned} I_1 = & (N^2 - N) \mathbb{E}[|h_{1i}| |h_{2i}| |h_{1j}| |h_{2j}| \cos(\phi_i - \phi_j)] \\ & + N \mathbb{E}[|h_{1i}|^2 |h_{2i}|^2]. \end{aligned} \quad (10)$$

By taking into account that $|h_{1i}|$, $|h_{2i}|$, $|h_{1j}|$, $|h_{2j}|$, and $\cos(\phi_i - \phi_j)$ are independent RVs with each other, I_1 can be rewritten as

$$\begin{aligned} I_1 = & (N^2 - N) \mathbb{E}[|h_{1i}|] \mathbb{E}[|h_{2i}|] \mathbb{E}[|h_{1j}|] \\ & \times \mathbb{E}[|h_{2j}|] \mathbb{E}[\cos(\phi_i - \phi_j)] + N \mathbb{E}[|h_{1i}|^2] \mathbb{E}[|h_{2i}|^2]. \end{aligned} \quad (11)$$

Moreover, considering that $|h_{1i}|$ and $|h_{2i}|$ are Nakagami- m distributed RVs and that ϕ is a uniformly distributed RV over $[-2^{-q}\pi, 2^{-q}\pi]$, after some algebraic manipulations, we derive that $\mathbb{E}[|h_{1i}|] = \mathbb{E}[|h_{2i}|] = \frac{\Gamma(m+1/2)}{\Gamma(m)} \left(\frac{\Omega}{m}\right)^{\frac{1}{2}}$, $\mathbb{E}[|h_{1j}|^2] = \mathbb{E}[|h_{2j}|^2] = \frac{\Gamma(m+1)}{\Gamma(m)} \left(\frac{\Omega}{m}\right)$ and $\mathbb{E}[\cos(\phi_i - \phi_j)] = \frac{4^q}{\pi} \sin^2\left(\frac{\pi}{2^q}\right)$, thus we can calculate I_1 as in (6). Similarly, by identifying the different terms of (9), we can obtain (7), thus enabling the calculation of m_t and Ω_t , which concludes the proof. ■

Next, we provide the ASEP for the considered RIS-assisted network for the case where s belongs to an M -ary HQAM constellation.

Proposition 2: For the case where s belongs to an M -ary HQAM, the ASEP of the considered RIS-assisted network can be tightly approximated as

$$P_a \approx \frac{2M-b}{2M} \left(\frac{\tilde{m}_t}{\tilde{m}_t + \frac{B}{\Omega_t} \bar{\gamma}} \right)^{\tilde{m}_t} + \frac{b}{M} P_1, \quad (12)$$

where $\bar{\gamma} = \frac{P_t G_{LP}}{\sigma_n^2}$, $\tilde{m}_t = \lfloor m_t \rfloor$, where $\lfloor \cdot \rfloor$ is the round function, and P_1 is given as

$$P_1 = \frac{1}{2} - \frac{1}{2} \sum_{z=0}^{m_t-1} \frac{m_t^z \sqrt{A^2 \bar{\gamma}} (2z)!}{(4\Omega_t)^z \sqrt{A^2 \bar{\gamma} + \frac{m_t}{\Omega_t} \left(\frac{A^2 \bar{\gamma}}{2} + \frac{m_t}{\Omega_t} \right)^z} z!}. \quad (13)$$

Proof: The ASEP for the considered RIS-assisted network for the case where M -HQAM is utilized is written as

$$P_a = \int_0^\infty P_s(x^2 \bar{\gamma}, k) f_x(x) dx. \quad (14)$$

By substituting (3) and (5) in (14), we obtain that

$$\begin{aligned} P_a = & \frac{(2M-b)m_t}{M\Gamma(m_t)\Omega_t^{m_t}} \int_0^\infty e^{-x^2(\bar{\gamma}B + \frac{m_t}{\Omega_t})} x^{2m_t-1} dx, \\ & + \frac{2bm_t}{M\Gamma(m_t)\Omega_t^{m_t}} \int_0^\infty Q(x\sqrt{\bar{\gamma}}A) x^{2m_t-1} e^{-\frac{m_t x^2}{\Omega_t}} dx. \end{aligned} \quad (15)$$

By utilizing the equation $Q(x) = \frac{1}{2} - \frac{1}{2} \text{erf}\left(\frac{x}{\sqrt{2}}\right)$, where $\text{erf}(\cdot)$ is the error function, and approximating m_t with $\lfloor m_t \rfloor$ the integrals in (15) can be calculated as in [10, (3.461/3)] and [11, (2.6.2/1)], which concludes the proof. ■

Next, we define the conditioned energy efficiency metric, which quantifies the network's energy efficiency under the condition that ASEP remains below a predefined threshold.

Definition 1: The conditioned energy efficiency of a wireless communication system that utilizes an M -ary constellation is defined as the ratio of the network's throughput to the network's energy consumption, under the condition that ASEP remains below a predefined threshold, and can be expressed as

$$E_c = U(P_f - P_v) \frac{(1 - P_f) B \log_2(M)}{P_c}, \quad (16)$$

where $U(\cdot)$ is the unit step function defined as $U(x) = 1$, if $x \geq 0$ and $U(x) = 0$, otherwise, P_f and B are the network's ASEP and bandwidth, respectively, P_v is the ASEP threshold, and P_c is the network's power consumption.

Considering the above definition, by substituting (12) in (16), the conditioned energy efficiency for the examined communication scenario is given as

$$E_c = U(P_a - P_v) \frac{(1 - P_a) B \log_2(M)}{P_t + P_{\text{ctr}} + qNP_{\text{PIN}}}, \quad (17)$$

where P_{ctr} is the power consumption of the RIS controller, and P_{PIN} is the power consumption of each PIN diode.

IV. DETECTION SCHEME

Incorporating HQAM into communication systems can significantly boost the system's energy efficiency. However, current research highlights that the detection algorithms for HQAM are more complex compared to those for traditional constellations (e.g., QAM), leading to a less favorable performance of HQAM in real-world applications. To address this issue, in this section, we introduce an innovative detection algorithm tailored for HQAM constellations that achieves a computational complexity of $\mathcal{O}(1)$, while maintaining performance levels comparable to the optimal maximum likelihood detection (MLD).

The key idea of our algorithm lies in identifying potential constellation symbols close to the received symbol $r = x_r + jy_r$, thereby reducing the necessary number of computed Euclidean distances between r and the constellation symbols. Within this framework, as in sphere decoding [12], we etch a circle centered on r with a radius of $R_m = d_{\min}$ and then define the regions $R_1 = [X_1, X_2]$ and $R_2 = [Y_1, Y_2]$, where X_1, X_2, Y_1 , and Y_2 are the tangent lines of the circle which are parallel to the axes, as illustrated in Fig. 2. The detection process is completed by obtaining the symbol $\hat{s} \in G = R_1 \cap R_2$ with the minimum Euclidean distance from r . To accomplish this, it becomes evident that we need to identify the constellation symbols that are contained within the region G . In this direction, we store all the real values x_i of the constellation symbols in ascending order within set S_x . Afterwards, we construct A_{x_i} , a two-column adjacent matrix for x_i , which is sorted in ascending order with respect to the values of its second column. In more detail, the first column enlists the constellation symbols with a real part equal to x_i , and the second column denotes their corresponding imaginary parts, and it is described as

$$A_{x_i} = \begin{bmatrix} s_{i,1} & \text{Im}(s_{i,1}) \\ \vdots & \vdots \\ s_{i,p} & \text{Im}(s_{i,p}) \end{bmatrix}, \quad (18)$$

where p denotes the number of symbols that their real part equals to x_i .

To design an $\mathcal{O}(1)$ detection algorithm tailored for HQAM constellations, it is essential to exploit their structure and the arrays S_x and A_x . In this direction, by noting that for an HQAM constellation the values in S_x and the values in the second column of A_x increase with a constant rate, we can formulate a linear interpolation function $f(\cdot)$ that returns the position of its input in the arrays, and thus, find the constellation symbols within G in $\mathcal{O}(1)$ time complexity. In particular,

when the input value u of f matches one of the array elements, f returns an integer value representing the position of u in the array. Conversely, if u is not an array element, f yields a non-integer value, where rounding this value results in the position of S_x with the closest corresponding value to u . Therefore, given that the elements of S_x are equispaced by $\frac{d_{\min}}{2}$ due to the HQAM geometry, we can define the linear interpolation function $f_x : \mathbb{R} \rightarrow \mathbb{R}$, which is given by

$$f_x(u) = \frac{2}{d_{\min}}u + 1 - \frac{2x_1}{d_{\min}}, \quad (19)$$

where x_1 is the first element of S_x . To this end, by utilizing (19), we can obtain the positions of the different $x_i \in S_x$ that satisfy $X_1 \leq x_i \leq X_2$, which are given as

$$\lceil f_x(X_1) \rceil \leq i \leq \lfloor f_x(X_2) \rfloor, \quad (20)$$

where $\lceil \cdot \rceil$ and $\lfloor \cdot \rfloor$ are the ceil and floor functions, respectively. In a similar manner, given that the elements of A_{x_i} are equispaced by $\frac{\sqrt{3}d_{\min}}{2}$ due to the HQAM geometry, we can also define the linear interpolation function $f_{\psi,i} : \mathbb{R} \rightarrow \mathbb{R}$, which is given by

$$f_{\psi,i}(v) = \frac{2}{\sqrt{3}d_{\min}}v + 1 - \frac{2A_{x_i}(1,2)}{\sqrt{3}d_{\min}}, \quad (21)$$

where $A_{x_i}(1,2)$ is the first element of the second column of the 2D matrix. Therefore, the j -th element of the second column of A_{x_i} that satisfies $Y_1 \leq \text{Im}(s_{i,j}) \leq Y_2$ can be obtained as

$$\lceil f_{\psi,i}(Y_1) \rceil \leq j \leq \lfloor f_{\psi,i}(Y_2) \rfloor. \quad (22)$$

Consequently, we can obtain the set S_c that contains the symbols within G which can be expressed as

$$S_c = \{s : s = A_{x_i}(j, 1)\}, \quad (23)$$

where $A_{x_i}(j, 1)$ is the j -th element of the first column of A_{x_i} . Finally, the symbol that the proposed detector determines is obtained by

$$\hat{s} = \arg \min_{s \in S_c} |r - s|^2. \quad (24)$$

It should be highlighted that $|S| \leq 6$ for any M -ary HQAM constellation, thus, instead of comparing M symbols, as the conventional MLD describes, we only need to calculate 6 Euclidean distances at most for any HQAM constellation.

To ensure that the aforementioned algorithm operates properly the region G must contain at least one symbol. However, under low-SNR conditions, it becomes quite possible that the received symbol is located far away from any other constellation symbol, thus, resulting in an empty region G . To tackle this, we initialize arrays Q_e , $e = \{1, 2, 3, 4\}$, with the external symbols of the constellation. These symbols are chosen such that at least a portion of their infinite decision region falls within the e -th quadrant of the 2D plane. Subsequently, when the received symbol r is situated in the e -th quadrant, we make a decision by selecting the symbol z from array Q_e with the smallest Euclidean distance to r . The time complexity of linearly traversing array Q_e to locate symbol z is $\mathcal{O}(\sqrt{M})$.

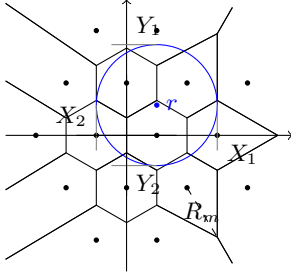


Fig. 2: Detection scheme of HQAM

Algorithm 1 Detection algorithm

Input: Coordinates of the received symbol r

Output: Detected symbol

- 1: Etch a circle with center r and radius R_m .
 - 2: Calculate points Y_1, Y_2 .
 - 3: Calculate points X_1, X_2 .
 - 4: $\hat{s} \leftarrow \text{null}$
 - 5: $S_c \leftarrow \text{null}$
 - 6: Q_e are initialized
 - 7: $x = f_x(S_x, X_1, X_2)$
 - 8: **for** x_i in x **do**
 - 9: $s_{i,c} = A_{x_i}(f_{\psi,i}(A_i(:, 2), Y_1, Y_2), 2)$
 - 10: APPEND($S_c, s_{i,c}$)
 - 11: **end for**
 - 12: **if** S_c is not null **then**
 - 13: $\hat{s} = \arg \min_{s \in S_c} |r - s|^2$
 - 14: **end if**
 - 15: **if** S_c is null **then**
 - 16: $e \leftarrow \text{quadrant of } r$
 - 17: $\hat{s} = \arg \min_{s \in Q_e} |r - s|^2$
 - 18: **end if**
 - 19: **return** \hat{s}
-

V. NUMERICAL RESULTS

In this section, we provide numerical results for the considered network and validate the derived analytical expressions via Monte Carlo simulations with 10^6 realizations. Specifically, we assume that the transmit power $P_t = 10^{-3}$ W, the reference distance d_0 is set at 1 m, while C_0 and σ_n^2 are set equal to -30 dBm and -140 dBm, respectively. Moreover, we assume that both BS and CN antennas are omnidirectional, i.e., $G_t = G_r = 1$, the path loss exponent n equals to 2.5, while the distances d_1 and d_2 are equal to 20 m and 60 m. In addition, both CN-RIS and RIS-BS links are assumed to be affected by Nakagami- m fading with shape parameter $m = 3$ and scale parameter $\Omega = 1$, respectively, whereas P_{ctr} and P_{PIN} are given equal to 50 mW and 1 mW.

In Figs. 3a and 3b, we present the ASEP of HQAM and QAM constellations for $M = 64$ and $M = 1024$, respectively. As it can be observed, the simulation results validate the tightness of the proposed ASEP approximation of an HQAM constellation, demonstrating the precision of our analysis. Moreover, it can be seen that the adoption of HQAM leads

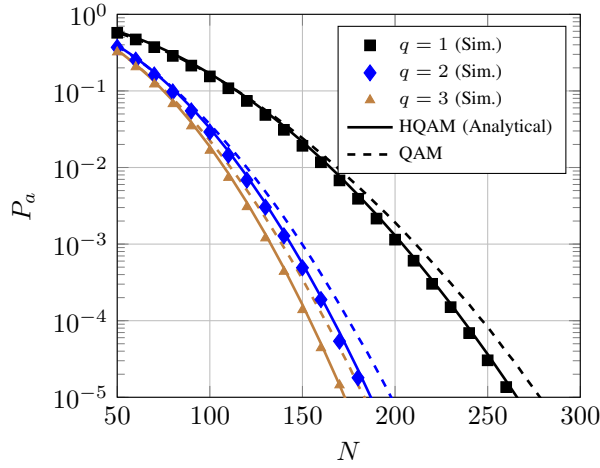
to a reduction in the number of required RIS elements, N , in comparison to conventional QAM, which enhances the cost-effectiveness of the system, as fewer reflecting elements are required. Additionally, as M increases, the superiority of HQAM compared to QAM becomes increasingly evident, attributed to the denser symbol allocation on the IQ plane, which enhances spatial efficiency. Furthermore, an increase in the quantization level, q , results in a decrease in the ASEP for both modulation schemes, indicating that a higher quantization level can improve network performance. However, the transition from $q = 1$ to $q = 2$ showcases a more significant performance gain than the progression from $q = 2$ to $q = 3$ for both $M = 64$ and $M = 1024$. Therefore, it becomes clear that increasing q beyond 2 is not a practical approach, as it fails to offer significant performance improvements and results in higher power consumption, highlighting the necessity for a cautious selection of q to enhance system performance and efficiency.

Fig. 4 illustrates the constrained energy efficiency E_c normalized to the network's bandwidth of HQAM and QAM constellations across varying q , considering a targeted ASEP of $P_u = 10^{-5}$. Notably, for all the examined q values, HQAM consistently requires a reduced number of reflecting elements to achieve the desired P_u , thus highlighting HQAM's contribution to energy efficiency enhancement. Furthermore, despite $q = 1$ showing the highest ASEP value for both HQAM and QAM, it is identified as the most favorable option in terms of E_c compared to $q = 2$ and $q = 3$, attributed to the significant rise in energy consumption that accompanies increasing q . Therefore, Fig. 4 underlines the importance of appropriate selection of q to not only meet performance criteria but also to minimize energy consumption, thus emphasizing the pivotal role of HQAM in achieving enhanced energy efficiency.

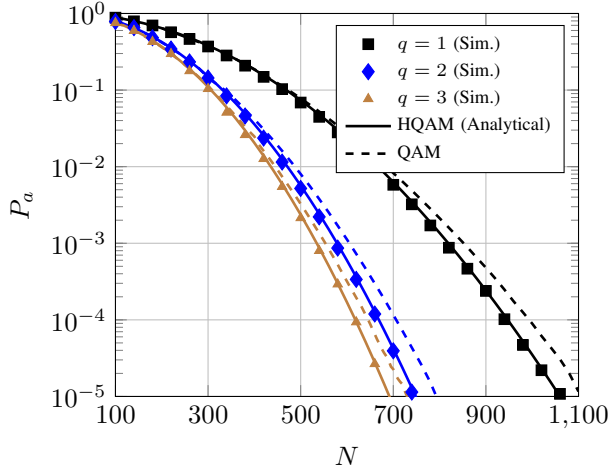
Finally, in Fig. 5, we show the detection accuracy of the proposed detection algorithm in comparison to the conventional MLD. Notably, the error rates in detection for the proposed approach are similar to those of MLD, thus our detection algorithm provides the same level of accuracy as MLD, while significantly reducing time complexity from $\mathcal{O}(M)$ to $\mathcal{O}(1)$. Consequently, our algorithm can assist in cases of large M , where the complexity of conventional MLD increases linearly with M , whereas the complexity of our algorithm remains constant regardless of the value of M .

VI. CONCLUSIONS

In this work, we explored the application of HQAM in RIS-assisted networks, focusing on its potential to minimize the number of reflecting elements. Specifically, we developed analytical expressions for the ASEP and introduced a novel metric for conditioned energy efficiency, assessing the network's energy efficiency while maintaining ASEP below a threshold value. Furthermore, we propose a novel detection algorithm for HQAM that implements sphere decoding in $\mathcal{O}(1)$ complexity. Our findings, validated through Monte Carlo simulations, highlighted HQAM's superiority in energy effi-



(a) $M = 64$



(b) $M = 1024$

Fig. 3: ASEP versus number of elements

ciency and ASEP over traditional QAM, offering significant insights for future wireless systems.

ACKNOWLEDGMENT

This work was funded from the Smart Networks and Services Joint Undertaking (SNS JU) under European Union's Horizon Europe research and innovation programme (Grant Agreement No. 101096456 - NANCY).

REFERENCES

- [1] M. Segata, P. Casari, M. Lestas, D. Tyrovolas *et al.*, "On the feasibility of RIS-enabled cooperative driving," in *Proc. IEEE Veh. Netw. Conf. (VNC)*, Istanbul, Turkey, Jun. 2023, pp. 143–150.
- [2] C. Liaskos, S. Nie, A. Tsioliaridou, A. Pitsillides, S. Ioannidis, and I. Akyildiz, "A new wireless communication paradigm through software-controlled metasurfaces," *IEEE Commun. Mag.*, vol. 56, no. 9, pp. 162–169, Sep. 2018.
- [3] E. Basar, M. Di Renzo, J. De Rosny, M. Debbah, M.-S. Alouini, and R. Zhang, "Wireless communications through reconfigurable intelligent surfaces," *IEEE Access*, vol. 7, pp. 116 753–116 773, Jun. 2019.
- [4] D. Tyrovolas, S. A. Tegos, V. K. Papanikolaou, Y. Xiao, P.-V. Mekikis *et al.*, "Zero-energy reconfigurable intelligent surfaces (zeRIS)," *IEEE Transactions on Wireless Communications*, pp. 1–1, 2023.

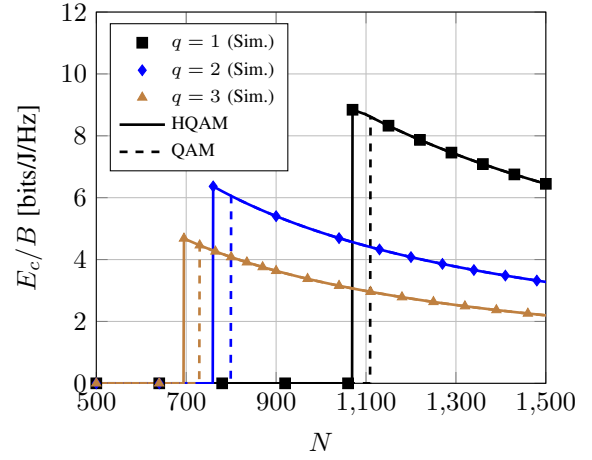


Fig. 4: Normalized E_c versus N for $M = 1024$

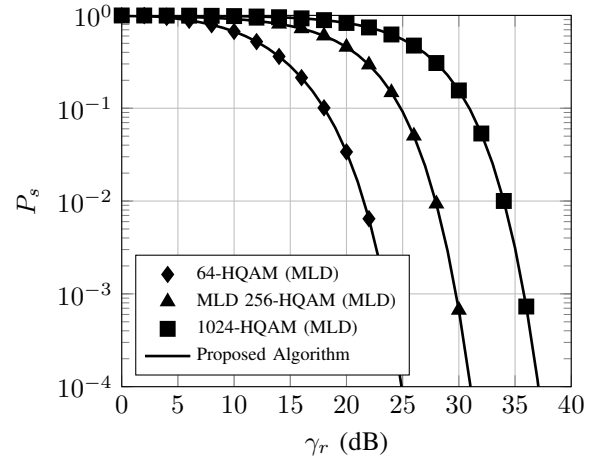


Fig. 5: Detected symbol error rate versus received SNR

- [5] P. K. Singya, P. Shaik, N. Kumar, V. Bhatia, and M.-S. Alouini, "A survey on higher-order qam constellations: Technical challenges, recent advances, and future trends," *IEEE Open J. Commun. Soc.*, vol. 2, pp. 617–655, Mar. 2021.
- [6] T. K. Oikonomou, S. A. Tegos, D. Tyrovolas, P. D. Diamantoulakis, and G. K. Karagiannidis, "On the error analysis of hexagonal-QAM constellations," *IEEE Commun. Lett.*, vol. 26, no. 8, pp. 1764–1768, Jun. 2022.
- [7] P. K. Singya, N. Kumar, V. Bhatia, and M.-S. Alouini, "On the performance analysis of higher order qam schemes over mixed RF/FSO systems," *IEEE Trans. Veh. Technol.*, vol. 69, no. 7, pp. 7366–7378, Apr. 2020.
- [8] H. Zhang, B. Di, L. Song, and Z. Han, "Reconfigurable intelligent surfaces assisted communications with limited phase shifts: How many phase shifts are enough?" *IEEE Trans. Veh. Technol.*, vol. 69, no. 4, pp. 4498–4502, Feb. 2020.
- [9] D. Tyrovolas, P.-V. Mekikis, S. A. Tegos, P. D. Diamantoulakis *et al.*, "On the performance of HARQ in IoT networking with UAV-mounted reconfigurable intelligent surfaces," in *Proc. IEEE Veh. Technol. Conf. (VTC)*, Helsinki, Finland, Jun. 2022, pp. 1–5.
- [10] I. S. Gradshteyn and I. M. Ryzhik, *Table of integrals, series, and products*. Academic press, 2014.
- [11] N. Korotkov and A. Korotkov, *Integrals Related to the Error Function*. CRC Press, 2020.
- [12] J. Jalden and B. Ottersten, "On the complexity of sphere decoding in digital communications," *IEEE Trans. on Signal Process.*, vol. 53, no. 4, pp. 1474–1484, 2005.